Applied Biochemistry and Biotechnology
https://doi.org/10.1007/s12010-021-03561-5

ORIGINAL ARTICLE

Co-immobilized Alcohol Dehydrogenase and Glucose Dehydrogenase with Resin Extraction for Continuous Production of Chiral Diaryl Alcohol

Jieyu Zhou[1] · Yanfei Wu[1] · Qingye Zhang[1] · Guochao Xu[1] · Ye Ni[1]

Received: 5 February 2021 / Accepted: 22 March 2021/Published online: 07 April 2021

Abstract

Ni^{2+}-functionalized porous ceramic/agarose composite beads (Ni-NTA Cerose) can be used as carrier materials to immobilize enzymes harboring a metal affinity tag. Here, a 6×His-tag fusion alcohol dehydrogenase Mu-S5 and glucose dehydrogenase from *Bacillus megaterium* (*Bm*GDH) were co-immobilized on Ni-NTA Cerose to construct a packed bed reactor (PBR) for the continuous synthesis of the chiral intermediate (*S*)-(4-chlorophenyl)-(pyridin-2-yl) methanol ((*S*)-CPMA) NADPH recycling, and in situ product adsorption was achieved simultaneously by assembling a D101 macroporous resin column after the PBR. Using an optimum enzyme activity ratio of 2:1 (Mu-S5: *Bm*GDH) and hydroxypropyl-β-cyclodextrin as co-solvent, a space-time yield of 1560 g/(L·d) could be achieved in the first three days at a flow rate of 5 mL/min and substrate concentration of 10 mM. With simplified selective adsorption and extraction procedures, (*S*)-CPMA was obtained in 84% isolated yield.

Keywords Flow reaction · Alcohol dehydrogenase · Co-immobilization · Diaryl ketone · In situ recovery

Introduction

In comparison to batch reactions, flow reactions are relatively new for biocatalytic preparation of value-added chemicals and active pharmaceutical ingredients, such as (*S*)-1-phenylethanol, (*R*)-flurbiprofen, and fatty acid methyl esters [1, 2]. In a flow reaction, fluid containing substrates are pumped to a reactor to produce a product stream [3–6]. When a flow process is applied to biocatalysis, it can be performed by using immobilized cells or enzymes [7–11]. As a continuous process, flow reactions have advantages of improved productivity, safety,

✉ Ye Ni
yni@jiangnan.edu.cn

[1] Key Laboratory of Industrial Biotechnology, Ministry of Education, School of Biotechnology, Jiangnan University, Wuxi 214122 Jiangsu, China

ease of modifying scale, and are especially useful for reactions with substrate/product inhibitory issues [12]. Additionally, downstream processing can become facile when using immobilized biocatalysts [13].

For coupling or multienzymatic reaction systems, co-immobilization is an ideal strategy. Co-immobilization could facilitate in situ removal of by-products and is essential for reactions that require cofactor regeneration [14, 15]. Therefore, it is critical to develop immobilization strategies favorable for preserving the activity of all involved enzymes. Additionally, the distribution of the enzyme on the support surface has a profound impact on the enzyme's overall biocatalytic activity [16]. Guián's group has developed an elegant approach in which they co-immobilize the main and recycling dehydrogenases on the same agarose-type support (activated with glyoxyl groups and metal chelates) [17]. Recently, this approach was adopted in a co-immobilized glycosyltransferase/sucrose synthase catalyzed system for NDP-glucose recycling [18].

Immobilized metal affinity chromatography (IMAC) has also been regarded as a potential strategy for enzyme co-immobilization. The IMAC strategy relies on coordination bonds between transition metal ions (such as Ni^{2+}, Cu^{2+}, Zn^{2+}, and Co^{2+}) and certain amino acids (such as His, Cys, and Trp) [19]. Co-expression of special fusion peptides results in specific coordinations between metal ions and proteins, giving advantages such as easy operation, target-specific purification, low activity loss, and recyclable carrier materials [20–24]. His-tag is one of the most popular fusion peptide for IMAC [25, 26]. In Böhmer and coworkers' study, a 6×His-tag fusion alcohol dehydrogenase (ADH) and amine dehydrogenase (AmDH) were co-immobilized on commercial metal-ion affinity glass beads EziG to produce chiral amine in batch reactions [27]. Additionally, Heli-tag, a metal-binding site (His-Ile-His-Asn-Leu-Asp-Cys-Pro-Asp-Cys) found in ATPase 439 from *Helicobacter pylori*, was identified to have strong metal affinity [28, 29]. The Heli-tag was reported to exhibit higher affinity than the 6×His-tag and has been successfully used for D-amino acid oxidase immobilization to obtain improved operational stability [30].

Notably, the co-immobilization strategies discussed above have mainly been applied in batch reactions. Additional aspects need to be considered when adopting co-immobilized enzymes in continuous reactions, such as operational stability and cofactor-recycling under flow mode. In a study by Dall'Oglio et al., chemical anchoring was adopted for co-immobilization of ADH and GDH to construct a continuous flow reactor. The stability of this system proved to be excellent during a 15-day operation run at a flow rate of 50 μL/min [31]. Peschke et al. constructed an all-enzyme hydrogel consisting of ADH and GDH using a self-assembling strategy, in which a stable bioconversion was operated for over 6 days at a flow rate of 10 μL/min [32]. However, activity loss caused by covalent anchors and insufficient structural rigidity of the all-enzyme hydrogel restricted the flow rate of the continuous reaction. Moreover, a continuous flow of cofactor was required in both studies. A regenerative electrochemical method [33, 34] and cofactor immobilization [35] have been reported for cofactor recycling in continuous flow biocatalysis; however, these studies were limited by complex immobilization procedures or reusability of immobilized carriers [36]. Given these limitations, we proposed a co-immobilization strategy for $NADP^+$/NADPH reutilization and regeneration with in situ product extraction in a continuous reaction.

In this study, a non-ionic adsorptive resin was used for $NADP^+$ recycling due to its specific adsorption of non-polar or low-polar organic compounds from aqueous solutions. Herein, we designed an $NADP^+$/NADPH regeneration strategy for a continuous flow reaction catalyzed by co-immobilized ADH/GDH. The asymmetric reduction of (4-chlorophenyl)(pyridine-2-yl)

ketone (CPMK) catalyzed by Mu-S5 (a mutant of *Kp*ADH from *Kluyveromyces polyspora*) [37, 38] was investigated as the model reaction. The chiral product (*S*)-(4-chlorophenyl)-(pyridin-2-yl) methanol [(*S*)-CPMA] is an important intermediate for synthesizing the anti-allergy drug bepotastine [38, 39]. *Bm*GDH from *Bacillus megaterium* was used for NADPH regeneration. The 6×His-tagged Mu-S5 and *Bm*GDH were co-immobilized on nickel-nitrilotriacetic acid-functionalized porous ceramic/agarose composite beads (Ni-NTA Cerose) to construct a packed bed reactor (PBR), which was followed by a D101 macroporous resin column. The feasibility of the proposed flow reaction process was validated by continuous synthesis and in situ recovery of (*S*)-CPMA.

Materials and Methods

Microorganisms and Chemicals

Recombinant *E. coli BL21* (DE3) strains harboring pET28-Mu-S5 and pET28-*Bm*GDH with *N*-terminal 6×His-tag were constructed in a previous study [38]. Ni-NTA Cerose was purchased from Qianchun Bio (Yancheng, China). Macroporous resins of D101 and XDA-1 and chelating rein IRC-748 were purchased from Lebiochem, Co. Ltd. (Xian, China). (4-Chlorophenyl)(pyridin-2-yl) methanone (CPMK) and all other reagents and solvents of analytical grade and biochemical reagents were obtained from Sinopharm Chemical Reagent Co. Ltd. (Shanghai, China).

Construction of N-terminal Heli-tagged Mu-S5

Plasmid pET28-Helitag-Mu-S5 was constructed by replacing the N-terminal 6×His-tag sequence in pET28-Mu-S5. Plasmid pET28-Mu-S5 was used as the template; 6×His-tag at N-terminal was replaced with Heli-tag by whole-plasmid PCR using KOD-Plus-Neo DNA polymerase purchased from Toyobo (Osaka, Japan). The following upstream and downstream primers were used:

Heli-tag-F: CATATTCATAATCTTGATTGTCCTGATTGTAGCAGCGGCCTGGTG

Heli-tag-R: ACAATCAGGACAATCAAGATTATGAATATGGCTGCTGCCCATGGT

The PCR protocol was as follows: 95 °C for 2 min, followed by 15 cycles of 94 °C for 30 s, 55 °C for 30 s, and 68 °C for 2.5 min. After *Dpn* I digestion at 37 °C for 30 min, the PCR products were transformed into competent *E. coli* BL21 (DE3) cells and plated onto Luria-Bertani agar plates supplemented with 50 μg/mL kanamycin.

Screening of Supporting Materials for Enzyme Immobilization

Preparation of the NTA Cerose Column

Each column (Φ = 72 mm, h = 24 mm) was packed with 1 mL of NTA Cerose and washed with 10 mL of deionized water followed by a solution of $NiSO_4$ or $MnCl_2$ (10 mL, 100 mM). The columns were then washed with 10 mL of deionized water to remove the unbound metal ions and equilibrated with 100 mM potassium phosphate buffer (pH 7.5). A ten-fold scale-up was used for the 10-mL Ni-NTA column.

Preparation of Reaction Solution

Solution A: For 1-mL PBR, a mixture solution containing 20% ethanol (v: v), 2 mM CPMK, 2 mM glucose, and 2 mM $NADP^+$ was prepared with 100 mM sodium phosphate buffer at pH 7.0. The mixture was warmed to 30 °C before use.

Solution B: For 10-mL PBR (after optimization), a mixture solution containing 20 mM hydroxypropyl-beta-cyclodextrin (HP-β-CD), 10 mM glucose, and 10 mM $NADP^+$ was prepared with 100 mM Tris-HCl buffer at pH 7.5. The mixture was incubated at 30 °C for 1 h, and then, CPMK (1 M in ethanol) was added to a final concentration of 10 mM.

Determination of the Amount of Immobilized Enzyme and Dilution Rate

Mn-NTA and Ni-NTA Creose columns (1 mL) were prepared as described above. First, Mu-S5 was purified by Ni affinity chromatography and desalinated by ultrafiltration centrifugation. The resultant purified Mu-S5 is obtained with specific activity of 6.64 U/mg (Table S1) and then diluted to around 10 U/mL (the actual value was determined to be 11.7 U/mL).

The amount of immobilized enzyme was measured by calculating the difference in enzyme activity between inflows and outflows. It is presumed that saturation adsorption was reached when total activity in outflows was 10% of the initial activity. The enzyme activities of inflows and outflows were measured following assay method described in analysis methods. The total activity of the immobilized enzyme was equal to the difference in total activity between inflows and outflows, and the amount of immobilized enzyme could be calculated by dividing by the specific activity of Mu-S5 (6.64 U/mg). The detailed data can be found in supplemental data (Table S2).

Dilution rate: According to the optimized results, the enzyme loading was 20 mg protein per mL of Ni-NTA Cerose (e.g., 16.7 mg protein/g Ni-NTA Cerose). Thus, 14.11 mg of purified Mu-S5 (94 U) and 5.89 mg of purified *Bm*GDH (47 U) were needed to construct a 1-mL PBR based on Ni-NTA/Mn-NTA Cerose. For operational convenience, 10 mg/mL solutions of both Mu-S5 and *Bm*GDH were prepared, corresponding to 1.41 mL and 0.596 mL loading volume, respectively. Then, a peristaltic pump was used to pump the reaction solution through the reactor at flow rates of 0.2, 0.4, 0.6, 0.8, and 1.0 mL/min. For a 10-mL Ni-NTA PBR, 141.1 mg (940 U) of Mu-S5 and 58.9 mg (470 U) of *Bm*GDH were mixed and loaded, and the flow rates were set at 2.0, 4.0, 6.0, 8.0, and 10 mL/min. All of the post-column effluents were collected separately and detected by HPLC.

$$\text{Dilution rate} = \frac{\text{Volumetric flow rate (mL/min)}}{\text{Reactor volume (mL)}}$$

Analysis Methods

Enzymatic Activity Assay

The activity of Mu-S5 and *Bm*GDH was spectrophotometrically determined according to the changes in absorption of NADPH or $NADP^+$ at 340 nm and 30 °C with a UV–Vis spectrophotometer using a molar extinction coefficient of 6220 M^{-1} cm^{-1}. For Mu-S5, the assay mixture contained 1.0 mM CPMK, 1.0 mM NADPH, and a proper amount enzyme in PBS

buffer (100 mM, pH 7.0). For *Bm*GDH, the assay mixture contained 1 mM D-glucose, 1 mM $NADP^+$, and 10 μL enzyme in PBS buffer (100 mM, pH 7.0). One unit of activity was defined as the amount of enzyme required for the depletion or production of 1.0 μmol of NADPH under the aforementioned conditions.

HPLC Analysis

The substrate conversion and *ee* value were determined using an Agilent 1100 HPLC system (USA) equipped with a Chiralcel OB-H column (0.46 mm × 250 mm, 5 μm, Diacel, Japan). The HPLC was performed at 254 nm using hexane:ethanol (95:5, v/v) as eluent at a flow rate of 0.8 mL/min.

Activity Recovery of Immobilized Mu-S5

Since spectrophotometric determination was not applicable for immobilized Mu-S5, the initial velocities of all entries were calculated using the substrate conversion from the first 10 min (substrate conversion < 20%) using an HPLC assay.

A purified Mu-S5 solution of 10 U/mL was prepared as described above. The Mu-S5 solutions (40 mL) were loaded on 1-mL Ni-NTA and Mn-NTA PBR columns, respectively. Enzymatic activity of inflows is performed in a 2-mL reaction mixture consisting of 10 mM CPMK, 10 mM NADPH, and 250 μL inflows in 100 mM PBS (pH 7.0) at 30 °C and 200 rpm for 10 min (Fig. S1 and Table S3).

The outflows are collected, and the enzymatic activity is determined in a 2-mL reaction mixture consisting of 10 mM CPMK, 10 mM NADPH, and 1 mL outflows in 100 mM PBS (pH 7.0) at 30 °C and 200 rpm for 10 min (Fig. S2 and Table S4).

The activity of immobilized Mu-S5 was determined as follows. Weight (in gram) rather than volume (in mL) was used to quantify immobilized Mu-S5. The total weights of 1 mL of immobilized enzymes (Mn-NTA and Ni-NTA Creose) were measured to be 1.23 and 1.20 g, respectively. Immobilized Mu-S5 was placed in a beaker containing 9 mL 100 mM PBS (pH 7.0) buffer. After mixing, 100 μL homogenized solution was transferred into 2.0-mL tubes followed by centrifugation. The liquid was then carefully removed, and the immobilized Mu-S5 was weighed. The activity of immobilized Mu-S5 is determined in a 2-mL reaction mixture consisting of 10 mM CPMK, 10 mM NADPH, and about 0.01 g of immobilized Mu-S5 in 100 mM PBS (pH 7.0) at 30 °C and 200 rpm for 10 min (Fig. S3 and Table S5). The data are summarized in Table S6.

$$\text{Activity recovery} = \frac{\text{Activity of immobilized enzyme}}{\text{Inflows activity-Outflows activity}} \times 100\%$$

2,4-Dinitrophenylhydrazine (DNPH) Assay

DNPH (2,4-dinitrophenylhydrazine) is a reagent used to detect the carbonyl of ketone or aldehyde functional groups. In this study, the formation of red dinitrophenylhydrazone with CPMK and DNPH substrates can be regarded as a positive result. First, DNPH was dissolved at 20 mM in ethanol containing 3% sulfuric acid and stored in darkness. Then, the chromogenic reaction was performed by addition of 100 μL of the DNPH solution into 100 μL of

effluent (after packed bed reactor). After standing for 15 min at 30 °C, 1 mL of KOH (0.5 M) was added, and the absorbance of the solution was determined at 500 nm by a microplate reader (Biotek, USA). Samples without CPMK were used as the control.

Bio-reduction Catalyzed by Immobilized Enzyme

Optimal pH and Temperature

Substrate conversion was performed in a 5-mL mixture containing Mu-S5 and *Bm*GDH (2 U each), 50 mM CPMK, and 50 mM glucose. The optimal pH of the reaction was determined by measuring the substrate conversion in the following buffers: sodium citrate-citric acid buffer (SCC buffer, pH 5.0–6.0, 100 mM), sodium phosphate buffer (pH 6.0–8.0, 100 mM), and Tris-HCl (pH 7.5–9.0, 100 mM). The optimal temperature was determined by measuring substrate conversion at 25–40 °C.

Optimal Ratio of Mu-S5 and BmGDH

A total dry mass of 2 mg purified Mu-S5 and *Bm*GDH were mixed at activity ratios of 10:1 to 1:10. The reaction mixture containing 100 mM CPMK, 100 mM glucose, premixed solutions of Mu-S5 and *Bm*GDH, and 100 mM Tris-HCl (pH 7.5) in a final volume of 5 mL was conducted at 30 °C for 30 min. The substrate conversion was analyzed by HPLC.

Effect of Various Co-solvents

In the pre-experiments, 10 mM CPMK was dissolved in different co-solvents. A mother solution of CPMK (1.0 M) was prepared in ethanol by heating. A volume of 10 μL CPMK mother solution (1.0 M) was added into different amounts of co-solvents, and then different volumes of water were added to a final volume of 1 mL (Tables S7 and S8). According to preliminary results, 5% Tween 80, 2.5% Triton X-100, and 20–40 mM HP-β-CD were tested as co-solvents. Substrate conversion was performed in a 5-mL mixture containing 0.2 U of Mu-S5 and 0.1 U of *Bm*GDH, 10 mM glucose, and 10 mM CPMK. The substrate conversion was analyzed by HPLC.

Extraction with Macroporous Resins

Static Adsorption/Desorption Rate of Macroporous Resins Toward CPMA

Adsorption rate Substrate CPMK in Solution B was replaced with the product (*S*)-CPMA to prepare Solution C. A mass of 0.5 g resin D101 or XDA-1 was added into 10 mL of Solution C; the adsorption process was then carried out at 30 °C and 150 rpm for 4 h; and the non-adsorbed (*S*)-CPMA was analyzed by HPLC.

$$\text{Adsorption rate} = \frac{\text{Initial concentration-Residual concentration}}{\text{Initial concentration}} \times 100\%$$

Desorption rate The 0.5 g masses of resin D101 or XDA-1 that had adsorbed (*S*)-CPMA were washed with water and filtered on a Buchner funnel. A volume of 10 mL ethanol or ethyl

acetate was added, and the desorption process was carried out at 30 °C and 150 rpm for 4 h. The concentration of (*S*)-CPMA in the desorbing agent was analyzed by HPLC.

$$\text{Desorption rate} = \frac{\text{Concentration in the desorbing agent}}{\text{Initial concentration}} \times 100\%$$

Adsorption Capacity of Macroporous Resins Toward $NADP^+$

A mass of 0.5 g resin D101 or XDA-1 was added to 10 mL of solution containing 10 mM $NADP^+$. The adsorption process was carried out at 30 °C and 150 rpm for 4 h, and the absorption capacity was determined using an EnzyChrom $NADP^+$/NADPH assay kit from BioAssay Systems (Hayward, CA).

Continuous Flow Reaction in a 10-mL PBR

A 12-mL polypropylene column was packed with 10 mL of Ni-NTA Cerose to prepare a PBR. A total of 200 mg of purified enzyme was loaded (141.1 mg Mu-S5 (940 U) and 58.9 mg *Bm*GDH (470 U)), and the enzyme loading was 20 mg protein/mL Ni-NTA Cerose (e.g., 16.7 mg protein/g Ni-NTA Cerose). For operational convenience, 50 mg/mL solutions of both Mu-S5 and *Bm*GDH were prepared, corresponding to 5.08 mL and 1.99 mL loading volumes, respectively. A peristaltic pump was used to pump Solution B through the PBR at 5 mL/min. A glass column filled with 28 g (40 mL) of resin D101 was connected to the PBR to extract CPMA from the effluent of the PBR.

A total of 4 L of reaction solution were prepared as described above. To ensure the continuity of the process, the 4 L initial reaction solution was divided into two portions (2 L each) for rotation. According to the dynamic adsorption capacity of macroporous resin D101, 5 columns (40 mL) filled with D101 were required to adsorb (*S*)-CPMA from 2 L of effluent. In this study, a fresh D101 column was changed every 80 min. Notably, D101 resin is reproducible and recyclable. After 400 min, 2 L of effluent solution was collected, and 2 mL CPMK solution (dissolved in ethanol at 1 M) was added as reaction solution for recycling. Meanwhile, the resin 101 that adsorbed (*S*)-CPMA in each column was collected and filtered with a Buchner funnel. A double volume (80 mL) of ethyl acetate was added, and the desorption process was carried out at 30 °C and 150 rpm for 4 h. The product (*S*)-CPMA was concentrated by rotary evaporation.

The space-time-yield (STY) was defined as the mass of (*S*)-CPMA produced per milliliter of PBR enzyme per day.

$$\text{STY} = \frac{\text{Amount of } (S)\text{-CPMA(g)}}{\text{Volume of PBR (L)} \times \text{Reaction time(d)}}$$

Treatment of Column Packing for Recovery and Reuse

After each batch process, the immobilized Ni-NTA Cerose was washed with 10 column volumes of 50 mM EDTA and water sequentially. After 30-min incubation with a solution

of 100 mM $NiSO_4$, the column was washed with 10 column volumes of water, and then reused for the next batch.

For the product adsorbent column, (*S*)-CPMA was collected by soaking with ethyl acetate, and then, the D101 macroporous resin was sequentially washed using a Buchner funnel with 2 column volumes of the following: a solution containing 95% ethanol, water, and 3% HCl; water (rinsed to neutral); a 3% NaOH solution; and water (rinsed to neutral).

Results and Discussion

Device for Enzyme Immobilization and Product Recovery

For continuous synthesis of (*S*)-CPMA, a prototype combined device consisting of four main parts is designed (Fig. 1), including a bottle of flow reaction solution (containing dissolved CPMK, $NADP^+$, and glucose), a PBR containing Ni-NTA Cerose with immobilized Mu-S5 and *Bm*GDH, a macroporous resin column for adsorbing hydrophobic products, and a beaker for effluent recovery. When the reaction solution flowed through the PBR, the ketone substrate CPMK was reduced into the corresponding chiral alcohol (*S*)-CPMA. After that, the hydrophobic (*S*)-CPMA would be adsorbed by the resin column, whereas the effluent solution containing residual water-soluble NAD(P)H/$NAD(P)^+$ and by-product gluconate would be collected for recovery. After replenishing CPMK and glucose, the effluent solution could be reused as reaction solution. The post-column samples of the PBR and the resin column were determined by using a previously established DNPH assay [37] to ensure complete bioreduction and adsorption. When the resin column reached saturation, it could easily be replaced with a new one, and the adsorbed (*S*)-CPMA could be separated from the resin by static or dynamic elution. This operation mode not only avoids the emulsification issue caused by extraction with organic solvents in biocatalytic reaction system but also allows for the reuse of expensive cofactors. Moreover, Ni-NTA Cerose could be recycled and reused by treatment with EDTA and $NiSO_4$ solutions after each batch. For the product adsorbent column, D101 macroporous resin is also recyclable and can be reused by treatment with dilute acid and alkali solutions. The whole process is simple and easy to operate with low material and downstream costs. Optimization of reaction conditions was performed to verify the feasibility of the continuous reaction process.

Screening of Supports for the Immobilization of Mu-S5 and *Bm*GDH

Immobilized metal affinity chromatography (IMAC) is commonly used for His-tagged protein purification and can also be applied to the immobilization of enzymes [25]. Herein, a commercially available NTA Cerose was chosen as the immobilization carrier material. Compared with the NTA agarose (0.05 Mpa/cm) commonly used in purification, NTA Cerose (1 Mpa/cm) possesses a stronger stability under system pressure and can withstand relatively higher flow rates. Ni^{2+} and Mn^{2+} are selected due to their positive effects on the catalytic activity of Mu-S5 (104% for Ni^{2+} and 116% for Mn^{2+}) (Fig. 2**a**). After immobilization, protein loading per gram carrier is calculated to be 61.9 mg for Ni-NTA Cerose and 42.2 mg for Mn-NTA Cerose (Table S2). Additionally, Ni-NTA Cerose and Mn-NTA Cerose maintained 58.0% and 66.4% relative catalytic activity compare with that of free enzyme in shake flasks, respectively (Table S6).

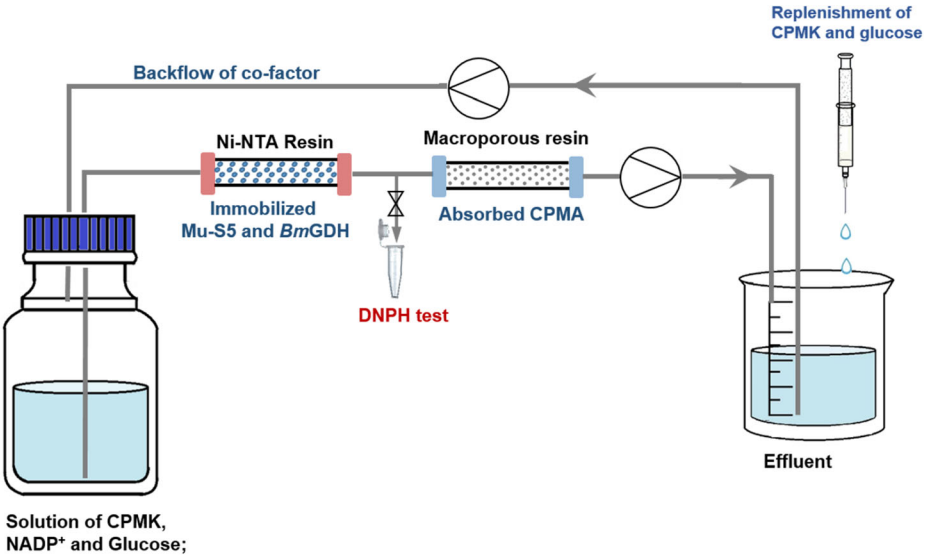

Fig. 1 Continuous biosynthesis of (*S*)-(4-chlorophenyl)-(pyridin-2-yl) methanol (*S*-CPMA) with immobilized Mu-S5 and *Bm*GDH and *in situ* product recovery

The dilution ratio was defined as the reactor volume divided by the volumetric flow rate of substrate, and it was used to evaluate the reactor performance. For Ni-NTA Cerose immobilized Mu-S5, the substrate conversion remained over 99% with increased substrate flow rate, whereas a consistent decline of conversion was observed for Mn-NTA Cerose. The conversion decreases to less than 50% at a flow rate of 1 mL/min for Mn-NTA (Fig. 2**b**). Due to the larger ionic radius of the Mn^{2+} ion (91 nm) compared to the Ni^{2+} ion (73 nm), the metal coordination bond strength of Ni^{2+} is stronger than that of Mn^{2+}. This difference in coordination bond strength is likely responsible for the poor performance of Mn-NTA. Notably, no protein leaching was detected at dilution rates of 0.2–1.0 min^{-1} as evaluated by a Bradford assay. Therefore, insufficient enzyme immobilized on Mn-NTA is likely responsible for the low conversion. To further reduce the cost, a cheaper chelating resin IRC-748 was functionalized with Ni^{2+} and employed for enzyme immobilization. However, activity above 85% was

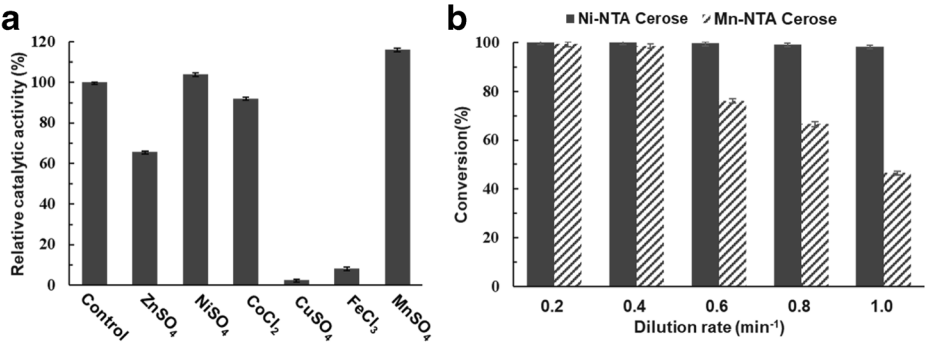

Fig. 2 Effect of metal ions on catalytic activity of Mu-S5 (**a**). Effect of dilution ratio on conversion ratio of Ni- and Mn-functionalized porous ceramic/agarose composite beads (Cerose) immobilized enzymes (**b**)

lost after immobilization due to the poor biocompatibility of the resin. Therefore, Ni-NTA Cerose was selected for protein immobilization.

Comparison of *6*×His-tag and Heli-tag in Protein Immobilization

In addition to the 6×His- tag, the Heli-tag fusion peptide with higher affinity was attempted for immobilization [28, 29]. Since the C-terminal portion of Mu-S5 is buried and solvent inaccessible, the Heli-tag was fused to the N-terminal of Mu-S5.

The affinity of 6×His- and Heli-tagged Mu-S5 with Ni-NTA is compared under the same elution conditions (Fig. 3). The two fused Mu-S5s showed similar solubility as confirmed by SDS-PAGE. Both fusion proteins were barely detected in the flow-through (lane 3). The majority of the 6×His-tag fused Mu-S5 eluted at 100 mM imidazole, and some was eluted at 50 mM imidazole (Fig. 3**b**). In contrast, almost all of the Heli-tag fused Mu-S5 is eluted at 20–50 mM imidazole (Fig. 3**a**). After elution with 50 mM imidazole, over 95% of enzymatic activity is lost with the of Heli-tag fused Mu-S5, whereas only 3.9% activity loss is observed with the 6×His-tag fused Mu-S5 (Table S9). It is speculated that the Heli-tag may not be fully exposed on the surface of Mu-S5, which may affect the structure and conformation of the protein [40]. Collectively, the Heli-tag that has been proven to be effective in D-amino acid oxidase immobilization [30] is not applicable for Mu-S5, and the 6×His-tag was used for enzyme immobilization for further study.

Optimization of Reaction Conditions of PBR

The reaction conditions were optimized to obtain improved catalytic performance. The pH, temperature, ratio of Mu-S5/*Bm*GDH, and co-solvent were optimized in shake flasks, and the dilution rate was determined in a PBR. As shown in Fig. 4**a**, Mu-S5 shows optimal activity at pH 7.5 in Tris-HCl buffer. The optimal temperature of the reaction is 30 °C (Fig. 4**b**), and the reaction can be conveniently performed at room temperature. Under the optimized pH and temperature, the highest conversion (75.1%) is achieved using immobilized Mu-S5/*Bm*GDH at

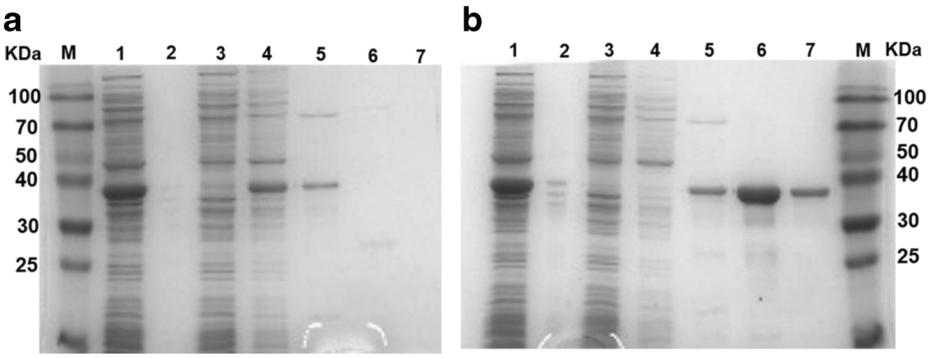

Fig. 3 SDS-PAGE of recombinant Mu-S5 fused with Heli-Tag (**a**) or 6×His Tag (**b**) eluted at different imidazole concentrations. (**a**) M: protein ladder; lane 1: supernatant of crude Heli-tag fused Mu-S5; lane 2: sediment of crude Heli-tag fused Mu-S5; lane 3: Flow-through of crude Heli-tag fused Mu-S5; lane 4-7: eluent from washing Heli-tag fused Mu-S5 with 20, 50, 100 and 300 mM imidazole, respectively; (B) M: protein ladder; lane 1: supernatant of crude 6×His-tag fused Mu-S5; lane 2: sediment of crude 6×His-tag fused Mu-S5; lane 3: Flow-through of crude 6×His-tag fused Mu-S5; lane 4-7: eluent from washing 6×His-tag fused Mu-S5 with 20, 50, 100 and 300 mM imidazole, respectively

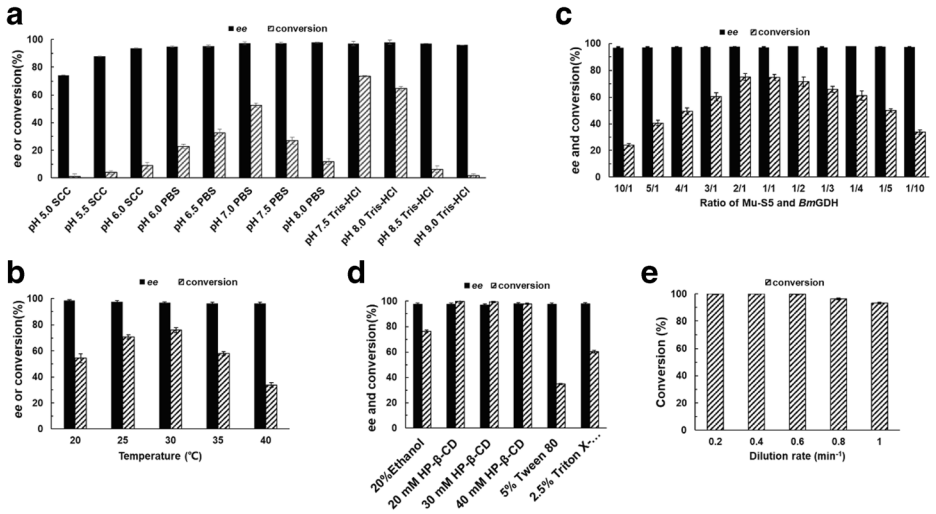

Fig. 4 Optimization of reaction catalyzed by immobilized Mu-S5 and *Bm*GDH. (**a**) pH; (**b**) temperature; (**c**) ratio of Mu-S5 and *Bm*GDH; (**d**) co-solvent; (**e**) flow rate optimum of (4-chlorophenyl)(pyridine-2-yl) ketone (CPMK) in a 10-mL Ni-functionalized porous ceramic/agarose composite beads (Ni-NTA Cerose) packed bed reactor

an activity ratio of 2:1 (Fig. 4**c**), which may be related to the addition of an equal amount of glucose as co-substrate. As there were not significant differences in the large-scale fermentation costs between Mu-S5 and *Bm*GDH (Table S1), the optimized activity ratio of 2:1 is acceptable.

Additionally, an aqueous solution of the insoluble substrate CPMK should be prepared for the continuous process. Several commonly used dispersants are screened, and a 10 mM aqueous solution of CPMK could be obtained when supplemented with 5% Tween 80, 2.5% Triton X-100, and 20 mM hydroxypropyl-beta-cyclodextrin (HP-β-CD) in preliminary experiments (Tables S7 and S8). Figure 4**d** shows the effect of co-solvents on catalytic activity of immobilized Mu-S5, and a reaction system with the addition of 20% ethanol served as a control. A decrease in substrate conversions was observed when using Tween 80 and Triton X-100 as co-solvents, and this may be attributed to the disrupted protein conformation that results from the interactions between the non-ionic surfactant and the hydrophobic region of the enzyme. Surprisingly, HP-β-CD not only improved the substrate solubility but also exhibited excellent biocompatibility. Benefiting from the hydrophilic exterior and hydrophobic interior structure of HP-β-CD, mass transfer was improved, and almost complete conversions were achieved with the addition of 20–40 mM HP-β-CD, whereas only 76.4% conversion was observed in the control reaction (20% ethanol). Finally, the dilution rate of 10-mL PBR ($\Phi = 1.6$ cm, $h = 5.5$ cm) was determined under the optimized reaction conditions. As shown in Fig. 4**e**, the substrate conversion began to decrease when the volumetric flow rate of CPMK exceeded 6 mL/min, and only 93.1% conversion was detected at an increased flow rate of 10 mL/min without protein leaching. Considering possible damage to the immobilized materials and enzymes caused by the long-term continuous reaction, a volumetric flow rate of 5 mL/min was chosen.

Comparison of Properties of D101 and XDA-1

Macroporous resins possess stable physical and chemical properties and can be classified into three types: polar, non-polar, and weakly polar. According to the design, the hydrophobic

diaryl alcohol product is expected to be adsorbed, whereas the water-soluble cofactor should be recycled and reused for consecutive reaction cycles. Therefore, two commonly used non-polar macroporous resins D101 and XDA-1 are selected for (*S*)-CPMA enrichment (Table S10). The adsorption rate is an important index to evaluate the adsorption performance of macroporous resins. As shown in Tables 1 and S11, the two resins maintain almost the same adsorption capacity toward the product (*S*)-CPMA. Resin XDA-1 with a larger surface area exhibited more than a 90% static adsorption rate. The desorption rate of the two resins toward (*S*)-CPMA is also compared (Table S12). Firstly, different proportions of recommended aqueous-ethanol were used as washing solutions; however, only about 20% of the product could be eluted even when pure ethanol (100%) was used. Then, ethyl acetate with lower polarity was tested, and the desorption rate increased rapidly. In the case of D101, more than 95% of CPMA could be eluted with the addition of ethyl acetate, whereas only 82.6% of CPMA could be eluted when XDA-1 was selected for extraction. Afterward, the residual $NADP^+$ concentration was measured using an $NADP^+$/NADPH assay kit to evaluate whether the selected resin could be used for coenzyme recycling. The results showe that neither D101 nor XDA-1 could adsorb $NADP^+$ (Table S13, Fig. S4). Thus, D101 was selected as the supporting material in the extraction column due to the higher desorption rate. Using a 40-mL column (Φ = 1.6 cm, h = 20 cm) filled with 28 g of D101 resin, fractions were collected sequentially every 10 mL, and a trace amount of (*S*)-CPMA was detected in the 47th sample. The dynamic adsorption capacity of D101 was calculated to be 36.3 mg/g, which is roughly equal to its static adsorption capacity (38.6 mg/g).

Asymmetric Synthesis and In Situ Extraction of (*S*)-CPMA in a Continuous Device

Asymmetric synthesis of (*S*)-CPMA is carried out under optimized immobilization and reaction conditions. Figure 5 shows the conversion ratio of CPMK catalyzed by immobilized Mu-S5/*Bm*GDH in a 10-mL PBR. A complete conversion of CPMK was observed in the first 3 days followed by a gradual decline. When the reaction proceeded to day 4, an obvious red brown color formed in DNPH assay, indicating an incomplete conversion of the ketone substrate. On day 7, only 54.3% conversion was observed by HPLC, and conversion continued to decrease sharply to 22.5% on day 8. In view of the negligible effect of the His-tag on protein structure, the insufficient stability of the Mu-S5 (half-life of 152 h at 30 °C, Fig. S5) might be responsible for the decreased substrate conversion after day 3. Finally, the STY was calculated to be 1560 g/(L·d) based on data from day 1 to 3. A total volume of 4 L initial reaction solution was recycled up to 6 times. After 400 min of reaction, the D101 resin in the first 5 adsorption columns was collected, and a total of 3.63 g (*S*)-CPMA with 84% isolated yield was obtained by ethyl acetate extraction.

Peschke et al. reported an emerging co-immobilization approach using *Spy*-tag and *Spy*-catcher fusion enzymes [32]. However, hydrogels self-assembled from free enzymes alone are

Table 1 Comparison of properties of D101 and XDA-1 resins

Resin	Constituent materials	Average aperture size (nm)	Specific surface area (m^2/g)	Static adsorption rate (%)	Desorption rate (%)
D101	Polystyrene	25–28	480–520	88.1 ± 0.13	96.1 ± 0.22
XDA-1	Polyacrylic acid	85–89	1000–1100	91.3 ± 0.08	82.7 ± 0.31

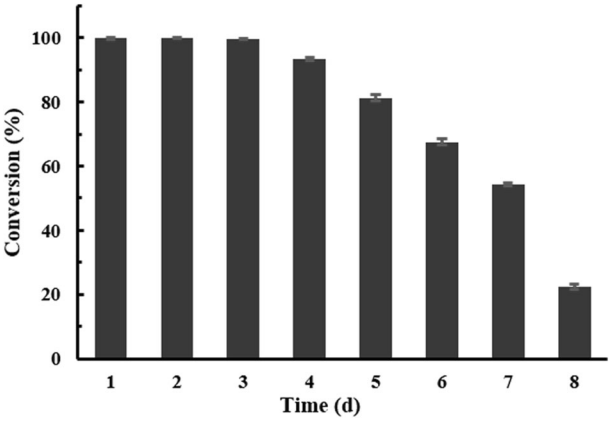

Fig. 5 Continuous production of (*S*)-(4-chlorophenyl)-(pyridin-2-yl) methanol (*S*-CPMA) in a 10-mL packed bed reactor

mechanically fragile, which limits the operation strength and flow rate of continuous reactions. In comparison, immobilized *Kp*ADH Mu-S5 and *Bm*GDH maintained excellent catalytic activity and operational stability under a 5 min^{-1} dilution rate during the first 3 days of the reaction. In a study by Dall'Oglio and coworkers, KRED1-Pglu and GDH were covalently bound to aldehyde-activated agarose [31]. Although the stability and solvent tolerance were improved, alkaline operating conditions (pH ≥ 10) pose a challenge to the catalytic activity of enzymes. For example, Tt-ADH2 and formate dehydrogenase (FDH) had to be immobilized by covalent binding and ionic adsorption, respectively, due to the inactivation of FDH after aldehyde immobilization [35]. In our study, ADH and GDH were both coordination bound to Ni-NTA Cerose, and over 60% of catalytic activity could be retained under near-neutral conditions (pH 7.5). Using commercially available enzyme membrane reactor, (*R*)-2-octanol could be continuously synthesized by co-immobilized *Lb*ADH and GDH, and produced a fairly high STY of 454 g/(L·d). Additionally, product separation and cofactor recycling are achieved by supercritical carbon dioxide ($scCO_2$) extraction [41] (Table 2).

In our study, the macroporous resin adsorption strategy with low equipment requirements was facilely used for product recovery, and in the subsequent resin extraction step, much less organic solvent was used than in traditional liquid-liquid extractions. Additionally, emulsification caused by proteins in free enzyme systems was completely avoided, and a satisfactory yield was obtained by the simple operations of soaking and rotary evaporation.

Conclusions

Continuous flow biocatalysis can improve the overall reaction process by protecting fragile enzymes from mechanical stirring or agitation, as well as simplifying the downstream product separation and treatment. Herein, a 6×His-tag fused Mu-S5 and *Bm*GDH were co-immobilized on Ni-NTA Cerose to construct a PBR for continuous asymmetric synthesis of (*S*)-CPMA. As a support material for enzyme immobilization, the commercially available Ni-NTA Cerose is recyclable in process operation, Furthermore, the D101 macroporous resin column was used after the PBR to adsorb the (*S*)-CPMA product specifically, and recycling and reuse of the reaction solution containing hydrophilic $NADP^+$/NADPH were easily achieved. During

Table 2 Comparison of asymmetric reductions catalyzed by various alcohol dehydrogenases (ADHs) and glucose dehydrogenases (GDHs)/formate dehydrogenases (FDHs) in flow reactions

	This study	Peschke et al. [32]	Dall'Oglio et al.[31]	Kohlmann et al.[41]	Velasco-Lozano et al [35]
Ketone reductase	Mu-S5 from *Kluyveromyces polyspora*	*Lb*ADH from *Lactobacillus brevis*	KRED1-Pglu from *Pichia glucozyma*	*Lb*ADH from *Lactobacillus brevis*	Tt-ADH2 from *Thermus thermophilus*
Cofactor recycling	GDH	GDH	GDH	GDH	FDH
Immobilized strategy	IMAC	Self-assembling;	Covalent binding	Interception by semi-permeable membrane	Covalent binding and ionic adsorption
Support material	Cerose	Hydrogel	Aldehyde-activated agarose	Enzyme membrane reactor	Aldehyde-activated agarose and polyethyleneimine agarose
Substrate	CPMK	5-Nitrononane-2,8-dione	1-Phenylpropane-1,2-dione	Octan-2-one	2,2,2-Trifluoro-1-phenylethanone
Conc.(mM)	10	5.0	3.0	6.0	5.0
Reactor volume (mL)	10	0.15	0.90	16	1.2
Flow rate (mL/min)	5.0	0.010	0.050	0.10	0.050
SYT (g/(L·d))	1560	≈100	4.4–81.5	454.5	62.7
In situ product recovery	Macroporous resins adsorption	No	No	scCO2 extraction.	No

400 min of flow reaction, a 4 L initial reaction solution could be recycled up to 6 times, demonstrating the feasibility of reducing the cost of cofactors. Additionally, the (*S*)-CPMA product was enriched on the D101 resin and could be separated conveniently and effectively by soaking in ethyl acetate. In summary, the designed continuous biocatalytic process using coupled PBR and in situ product recovery could be potentially applied in preparation of chiral alcohols. This continuous flow biocatalysis system is especially suitable for enzymatic reactions involving cofactor recycling and substrate/product inhibitory issues.

Abbreviations *ADH,* Alcohol dehydrogenase; *GDH,* Glucose dehydrogenase; *FDH,* Formate dehydrogenase; *CPMK,* (4-Chlorophenyl)(pyridine-2-yl)ketone; *(S)-CPMA,* (*S*)-(4-Chlorophenyl)-(pyridin-2-yl) methanol; *DNPH,* 2,4-Dinitrophenylhydrazine; *PBR,* Packed bed reactor; *Cerose,* Ceramic/agarose composite beads

Supplementary Information The online version contains supplementary material available at https://doi.org/10.1007/s12010-021-03561-5.

Authors' Contributions Jieyu Zhou: Conceptualization, investigation, methodology, writing-original draft. Yanfei Wu: Data curation. Qingye Zhang: Data curation, formal analysis. Guochao Xu: Writing—review and editing. Ye Ni: Supervision, writing—review and editing, project administration, funding acquisition.

Funding This work was supported by the National Key R&D Program [2018YFA0901700], the National Natural Science Foundation of China [21907040, 21776112, 22077054], China Postdoctoral Science Foundation [2019 M651703], the National First-Class Discipline Program of Light Industry Technology and Engineering [LITE2018-07], and the Program of Introducing Talents of Discipline to Universities [111-2-06].

Declarations

Competing Interests The authors declare no competing interests.

References

1. Britton, J., Majumdar, S., & Weiss, G. A. (2018). Continuous flow biocatalysis. *Chemical Society Reviews, 47*(15), 5891–5918.
2. Adamo, A., Beingessner, R. L., Behnam, M., Chen, J., Jamison, T. F., Jensen, K. F., Monbaliu, J. M., Myerson, A. S., Revalor, E. M., Snead, D. R., Stelzer, T., Weeranoppanant, N., Wong, S. Y., & Zhang, P. (2016). *Science, 352*, 54–61.
3. Webb, D., & Jamison, T. F. (2010). Continuous flow multi-step organic synthesis. *Chemical Science, 1*(6), 675–680.
4. Cuong, N. P., Lee, W., Oh, I., Thuy, N. M., Kim, D., Park, J., & Park, K. (2016). Continuous production of pure maltodextrin from cyclodextrin using immobilized Pyrococcus furiosus thermostable amylase. *Process Biochemistry, 51*(2), 282–287.
5. Cimporescu, A., Todea, A., Badea, V., Paul, C., & Peter, F. (2016). Efficient kinetic resolution of 1,5-dihydroxy-1,2,3,4-tetrahydronaphthalene catalyzed by immobilized Burkholderia cepacia lipase in batch and continuous-flow system. *Process Biochemistry, 51*(12), 2076–2083.
6. Jia, C., Wang, H., Zhang, W., Zhang, X., & Feng, B. (2018). Efficient enzyme-selective synthesis of monolauryl mannose in a circulating fluidized bed reactor. *Process Biochemistry, 66*, 28–32.
7. de Oliveira Lopes, R., Ribeiro, J. B., Silva De Miranda, A., Vieira Da Silva, G. V., Miranda, L. S. M., Ramos Leal, I. C., & Mendonça Alves De Souza, R. O. (2014). *Tetrahedron, 70*, 3239–3242.
8. Tamborini, L., Romano, D., Pinto, A., Contente, M., Iannuzzi, M. C., Conti, P., & Molinari, F. (2013). Biotransformation with whole microbial systems in a continuous flow reactor: resolution of (RS)-flurbiprofen using Aspergillus oryzae by direct esterification with ethanol in organic solvent. *Tetrahedron Letters, 54*(45), 6090–6093.

9. Döbber, J., Gerlach, T., Offermann, H., Rother, D., & Pohl, M. (2018). Closing the gap for efficient immobilization of biocatalysts in continuous processes: HaloTag™ fusion enzymes for a continuous enzymatic cascade towards a vicinal chiral diol. *Green Chemistry, 20*(2), 544–552.
10. Xiao, M., Qi, C., & Obbard, J. P. (2011). *Bioenergy, 3*, 293–298.
11. Tan, A. W., Fischbach, M., Huebner, H., Buchholz, R., Hummel, W., Daussmann, T., Wandrey, C., & Liese, A. (2006). Synthesis of enantiopure (5R)-hydroxyhexane-2-one with immobilised whole cells of Lactobacillus kefiri. *Applied Microbiology and Biotechnology, 71*(3), 289–293.
12. Thompson, M. P., Peñafiel, I., Cosgrove, S. C., & Turner, N. J. (2018). *Organic Process Research and Development, 23*, 9–18.
13. Li, F., Zheng, Y., Li, H., Chen, F., Yu, H., & Xu, J. (2019). Preparing β-blocker (R)-Nifenalol based on enantioconvergent synthesis of (R)-p-nitrophenylglycols in continuous packed bed reactor with epoxide hydrolase. *Tetrahedron, 75*(12), 1706–1710.
14. Orrego, A. H., López-Gallego, F., Espaillat, A., Cava, F. M. J., & A, G.A.A.J. (2018). *ChemCatChem, 10*, 3002–3011.
15. García-García, P., Rocha-Martin, J., Fernandez-Lorente, G., & Guisan, J. M. (2018). *Enzyme and Microbial Technology, 115*, 73–80.
16. Arana-Pena, S., Carballares, D., Morellon-Sterlling, R., Berenguer-Murcia, A., Alcantara, A. R., Rodrigues, R. C., & Fernandez-Lafuente, R. (2020). Enzyme co-immobilization: Always the biocatalyst designers' choice…or not? *Biotechnology Advances, 107584*. https://doi.org/10.1016/j.biotechadv.2020.107584.
17. Rocha-Martín, J., Rivas, B. D. L., Muñoz, R., Guisán, J. M., & López-Gallego, F. (2012). Rational Co-Immobilization of Bi-Enzyme Cascades on Porous Supports and their Applications in Bio-Redox Reactions with In Situ Recycling of Soluble Cofactors. *ChemCatChem, 4*(9), 1279–1288.
18. Trobo-Maseda, L., Orrego, A. H., Guisan, J. M., & Rocha-Martin, J. (2020). Coimmobilization and colocalization of a glycosyltransferase and a sucrose synthase greatly improves the recycling of UDP-glucose: Glycosylation of resveratrol 3-O-β-D-glucoside. *International Journal of Biological Macromolecules, 157*, 510–521.
19. Hearon, J. Z., Sundberg, L., & MalmstrOm, B. G. (1975). *Nature, 258*, 598–599.
20. Planchestainer, M., Contente, M. L., Cassidy, J., Molinari, F., Tamborini, L., & Paradisi, F. (2017). Continuous flow biocatalysis: production and in-line purification of amines by immobilised transaminase from Halomonas elongata. *Green Chemistry, 19*(2), 372–375.
21. Liu, J., Pang, B. Q. W., Adams, J. P., Snajdrova, R., & Li, Z. (2017). Coupled Immobilized Amine Dehydrogenase and Glucose Dehydrogenase for Asymmetric Synthesis of Amines by Reductive Amination with Cofactor Recycling. *ChemCatChem, 9*(3), 425–431.
22. Vahidi, A. K., Yang, Y., Ngo, T. P. N., & Li, Z. (2015). Simple and Efficient Immobilization of Extracellular His-Tagged Enzyme Directly from Cell Culture Supernatant As Active and Recyclable Nanobiocatalyst: High-Performance Production of Biodiesel from Waste Grease. *ACS Catalysis, 5*(6), 3157–3161.
23. Yang, J., Ni, K., Wei, D., & Ren, Y. (2015). One-step purification and immobilization of his-tagged protein via Ni2+-functionalized Fe3O4@polydopamine magnetic nanoparticles. *Biotechnology and Bioprocess Engineering, 20*(5), 901–907.
24. Engelmark Cassimjee, K., Kadow, M., Wikmark, Y., Svedendahl Humble, M., Rothstein, M. L., Rothstein, D. M., & Bäckvall, J. E. (2014). A general protein purification and immobilization method on controlled porosity glass: biocatalytic applications. *Chemical Communications, 50*(65), 9134.
25. Ueda, E. K. M., Gout, P. W., & Morganti, L. (2003). Current and prospective applications of metal ion–protein binding. *Journal of Chromatography. A, 988*(1), 1–23.
26. Chou, Y., Ko, C., Chen, L. O., & Shaw, C. Y. (2015). Purification and Immobilization of the Recombinant Brassica oleracea Chlorophyllase 1 (BoCLH1) on DIAION®CR11 as Potential Biocatalyst for the Production of Chlorophyllide and Phytol. *Molecules, 20*(3), 3744–3757.
27. Böhmer, W., Knaus, T., & Mutti, F. G. (2018). Hydrogen-Borrowing Alcohol Bioamination with Coimmobilized Dehydrogenases. *ChemCatChem, 10*(4), 731–735.
28. Melchers, K., Herrmann, L., Mauch, F., Bayle, D., Heuermann, D., Weitzenegger, T., Schuhmacher, A., Sachs, G., Haas, R., Bode, G., Bensch, K., & Schäfer, K. P. (1998). *Acta Physiologica Scandinavica. Supplementum, 643*, 123–135.
29. Melchers, K., Weitzenegger, T., Buhmann, A., Steinhilber, W., Sachs, G., & Schafer, K. P. (1996). Cloning and Membrane Topology of a P type ATPase from Helicobacter pylori. *The Journal of Biological Chemistry, 271*(1), 446–457.
30. Hou, J., Jin, Q., Du, J., Li, Q., Yuan, Q., & Yang, J. (2014). A rapid in situ immobilization of d-amino acid oxidase based on immobilized metal affinity chromatography. *Bioprocess and Biosystems Engineering, 37*(5), 857–864.

31. Dall'Oglio, F., Contente, M. L., Conti, P., Molinari, F., Monfredi, D., Pinto, A., Romano, D., Ubiali, D., Tamborini, L., & Serra, I. (2017). Flow-based stereoselective reduction of ketones using an immobilized ketoreductase/glucose dehydrogenase mixed bed system. *Catalysis Communications, 93*, 29–32.
32. Peschke, T., Bitterwolf, P., Gallus, S., Hu, Y., Oelschlaeger, C., Willenbacher, N., Rabe, K. S., & Niemeyer, C. M. (2018). *Angewandte Chemie, International Edition, 57*, 17028–17032.
33. Fassouane, A., Laval, J. M., Moiroux, J., & Bourdillon, C. (1990). Electrochemical regeneration of NAD in a plug-flow reactor. *Biotechnology and Bioengineering, 35*(9), 935–939.
34. Ruinatscha, R., Buehler, K., & Schmid, A. (2014). Development of a high performance electrochemical cofactor regeneration module and its application to the continuous reduction of FAD. *Journal of Molecular Catalysis B: Enzymatic, 103*, 100–105.
35. Velasco-Lozano, S., Benítez-Mateos, A. I., & López-Gallego, F. (2017). *Angewandte Chemie, International Edition, 56*, 771–775.
36. Benítez-Mateos, A. I., San Sebastian, E., Ríos-Lombardía, N., Morís, F., González-Sabín, J., & López-Gallego, F. (2017). Asymmetric Reduction of Prochiral Ketones by Using Self-Sufficient Heterogeneous Biocatalysts Based on NADPH-Dependent Ketoreductases. *Chemistry - A European Journal, 23*(66), 16843–16852.
37. Zhou, J., Xu, G., Han, R., Dong, J., Zhang, W., Zhang, R., & Ni, Y. (2016). Carbonyl group-dependent high-throughput screening and enzymatic characterization of diaromatic ketone reductase. *Catalysis Science & Technology, 6*(16), 6320–6327.
38. Zhou, J., Wang, Y., Xu, G., Wu, L., Han, R., Schwaneberg, U., Rao, Y., Zhao, Y., Zhou, J., & Ni, Y. (2018). Structural Insight into Enantioselective Inversion of an Alcohol Dehydrogenase Reveals a "Polar Gate" in Stereorecognition of Diaryl Ketones. *Journal of the American Chemical Society, 140*(39), 12645–12654.
39. Ni, Y., Zhou, J., & Sun, Z. (2012). Production of a key chiral intermediate of Betahistine with a newly isolated Kluyveromyces sp. in an aqueous two-phase system. *Process Biochemistry, 47*(7), 1042–1048.
40. Gaberc-Porekar, V., & Menart, V. (2001). Perspectives of immobilized-metal affinity chromatography. *Journal of Biochemical and Biophysical Methods, 49*(1-3), 335–360.
41. Kohlmann, C., Leuchs, S., Greiner, L., & Leitnera, W. (2011). Continuous biocatalytic synthesis of (R)-2-octanol with integrated product separation. *Green Chemistry, 13*(6), 1430–1437.